Med Chem Res
DOI 10.1007/s00044-015-1478-6

MEDICINAL CHEMISTRY RESEARCH

ORIGINAL RESEARCH

Synthesis, antimicrobial activities and QSAR studies of heterocyclic Schiff base ligands with organosilicon(IV) halides

Jai Devi[1] · Suman Kumari[1] · Nisha Batra[1] · Pradeep Kumar[2] · Balasubramanian Narasimhan[2] · Rajesh Malhotra[1]

Received: 26 February 2015 / Accepted: 1 November 2015

Abstract A series of heterocyclic Schiff base ligands 4-hydroxy-3-[1-{(2-hydroxy-aryl) imino}-ethyl]-6-methyl-pyran-2-one; aryl = phenyl, 4-methylphenyl, 4-chlorophenyl or 4-nitrophenyl (**1–4**) and their organosilicon(IV) complexes $R_2Si(L)$ (R = Et, Bu or Ph) (**5–16**) were synthesized and characterized. The elemental analyses, molar conductance and spectral (IR, ^1H, ^{13}C and ^{29}Si NMR) data suggested pentacoordinated environment around the silicon atom, where tridentate ligands coordinate through the azomethine nitrogen and oxygen of hydroxyl groups. The ligands and their organosilicon complexes were tested in vitro against pathogenic bacteria and fungi to assess their antimicrobial properties. The activity of the ligands improved against most of the strains of the tested microorganisms on complexation to the organosilicon groups. The antimicrobial activities were correlated with QSAR studies using the linear free energy relationship model which indicate the importance of topological parameters, third-order and valence first-order molecular connectivity indices ($^3\chi^v$ and $^1\chi^v$), to explain the antibacterial and antifungal activities of all synthesized compounds.

Keywords Organosilicon complexes · Dehydroacetic acid · Antimicrobial activity · Heterocyclic ligand · QSAR

Introduction

The Schiff base complexes are of particular interest to inorganic chemists for their structural, spectral and chemical behaviour (Raman *et al.*, 2007; Malhotra *et al.*, 2007; Devi *et al.*, 2012a). Many of these complexes provide biological models for understanding the structure of biomolecules and biological processes which are of special interest to bioinorganic chemists (Bharti *et al.*, 2010). Schiff bases and their silicon complexes exhibit a broad spectrum of biological activity such as antibacterial, antifungal, antitumor, antiviral, anti-inflammatory, insecticidal and antinematodal because of their specific structures (Jain *et al.*, 2004; Belwal and Singh, 2000; Singh and Dharampal, 2009; Abad *et al.*, 2004). It is, however, noteworthy that the biological activity is enhanced on complexation to silicon atoms (Devi *et al.*, 2012b). It has been reported that some microorganisms have already become resistant to many of the commonly used organic drugs. Therefore, today's requirement for researchers is to develop novel antibacterial and antifungal drugs which would target the lipid layer of microorganisms. Earlier we have reported that when biological active molecule is attached to the metal atom, the lipophilic nature is increased which favours its permeation through the lipid layer of the cell membrane of the microorganisms thus interfering the cell process (Devi *et al.*, 2012c; Devi and Batra, 2013; Yousef *et al.*, 2012).

Quantitative structure–activity relationship (QSAR) models are effective in describing structural basis of

Electronic supplementary material The online version of this article (doi:10.1007/s00044-015-1478-6) contains supplementary material, which is available to authorized users.

✉ Rajesh Malhotra
malhotra_ksrk@yahoo.co.in

[1] Department of Chemistry, Guru Jambheshwar University of Science and Technology, Hisar, Haryana 125001, India

[2] Faculty of Pharmaceutical Sciences, Maharishi Dayanand University, Rohtak, Haryana 124001, India

Published online: 07 November 2015

biological activity of chemical compounds by using computer-aided models. Previous studies in the field of QSAR (Judge *et al.*, 2012; Kumar *et al.*, 2012) indicated that the multi-target QSAR (mt-QSAR) models are better than one-target QSAR (ot-QSAR) models in describing the antimicrobial activity. So, in the present study, we have developed multi-target QSAR models to describe the antimicrobial activity of synthesized compounds. In the present work, dehydroacetic acid is used as one component for the synthesis of Schiff base ligands which were reported to act as fungicides and bactericides (Munde *et al.*, 2010). So, we hereby report synthesis, characterization, antimicrobial evaluation and QSAR studies of Schiff base ligands and their organosilicon(IV) complexes.

Materials and methods

Analytical grade dichlorodiorganosilane and 2-aminophenol derivatives were purchased from Aldrich. Solvents were purified according to standard procedures (Vogel, 1999). Anhydrous conditions were maintained throughout during the synthesis of the complexes, since the dichlorodiorganosilane and their product complexes are highly moisture sensitive. Molar conductances were measured in dry DMSO with a conductivity bridge model-306 Systronics. Silicon was estimated gravimetrically as SiO_2. The IR spectra were recorded using a Spectrum BX Series FT-IR spectrophotometer using KBr pellets. Multinuclear magnetic resonance spectra (^1H, ^{13}C, ^{29}Si) were recorded on a Bruker Avance II 300-MHz NMR Spectrometer, and all chemical shifts δ were reported in ppm relative to tetramethylsilane (TMS) as an internal standard in $CDCl_3$ and DMSO-d_6. Elemental analyses were carried out on a Perkin Elmer 2400. Mass spectra were recorded on an API 2000 (Applied Biosystems) mass spectrometer equipped with an electrospray source and a Shimadzu prominence LC. All the bacterial strains were procured from Microbial Type Culture Collection (MTCC), IMTECH, Chandigarh.

Experimental

*General procedure for the synthesis of ligands (**1–4**)*

The synthesis of the ligand, 4-hydroxy-3-[1-(2-hydroxy-phenylimino)-ethyl]-6-methyl-pyran-2-one (H_2L_I), was carried out by dissolving 1.68 g dehydroacetic acid (10 mmol) in 20 mL of ethanol and 1.23 g 4-methyl-2-aminophenol (10 mmol) in 10 mL of the ethanol separately. The solutions were mixed together and refluxed for 30 min. After cooling, a brownish precipitate formed at room temperature was recrystallized from ethanol to give the pure compound. Similarly, the reactions between dehydroacetic acid and substituted 2-aminophenol yielded the other Schiff base ligands ($H_2L_{I–IV}$).

H_2L_I (1): brown (EtOH); yield: 80 %; IR (KBr) ν max 3380, 1605 cm^{-1}; ^1H NMR ($CDCl_3$, 300 MHz,): δ = 10.57 (1H, C_4–OH), 15.23 (1H, C_9–OH), 5.59 (1H, C_5–H), 7.44 (d, J = 8.5 Hz, 1H), 7.29 (s, 1H), 7.02 (d, J = 8.5 Hz, 1H); ^{13}C NMR ($CDCl_3$, 300 MHz): δ = 163.4 (C, C_2), 96.2 (C, C_3), 182.3 (C, C_4), 105.1 (C, C_5), 162.9 (C, C_6), 176.1 (C, C_7), 19.5, 19.0 (C–CH_3), 149.1, 130.4, 126.9, 125.2, 123.7 117.1 (Ar–C); MS *m/z*: 260.0 $C_{14}H_{13}NO_4$ (calcd. 259.2); Anal. Calcd: C, 64.86; H, 5.05; N, 5.40. Found: C, 64.98; H, 5.35; N, 5.64.

H_2L_{II} (2): light brown (EtOH); yield: 81 %; IR (KBr) ν max 3390, 1620 cm^{-1}; ^1H NMR ($CDCl_3$, 300 MHz,): δ = 8.32 (1H, C_4–OH), 14.98 (1H, C_9–OH), 5.70 (1H, C_5–H), 7.10 (d, J = 8.4 Hz, 1H), 6.98 (d, J = 8.4 Hz, 1H), 6.85 (s 1H); ^{13}C NMR ($CDCl_3$, 300 MHz): δ = 163.8 (C, C_2), 96.5 (C, C_3), 183.8 (C, C_4), 106.4 (C, C_5), 162.1 (C, C_6), 175.5 (C, C_7), 19.7, 19.1 (C–CH_3), 150.2, 128.8, 126.3, 124.4, 122.3 117.6 (Ar–C); MS *m/z*: 274.4 $C_{15}H_{15}NO_4$ (calcd. 273.2); Anal. Calcd: C, 65.92; H, 5.53; N, 5.13. Found: C, 66.12; H, 5.82; N, 5.35.

H_2L_{III} (3): dark brown (EtOH); yield: 78 %; IR (KBr) ν max 3385, 1619 cm^{-1}; ^1H NMR ($CDCl_3$, 300 MHz,): δ = 9.99 (1H, C_4–OH), 15.38 (1H, C_9–OH), 5.81 (1H, C_5–H), 7.06 (d, J = 9.6 Hz, 1H), 7.03 (s, 1H), 6.90 (d, J = 9.6 Hz, 1H); ^{13}C NMR ($CDCl_3$, 300 MHz): δ = 163.7 (C, C_2), 96.5 (C, C_3), 183.9 (C, C_4), 106.8 (C, C_5), 162.7 (C, C_6), 176.3 (C, C_7), 19.6, 18.9 (C–CH_3), 151.2, 128.1, 127.1, 123.9, 121.9 118.1 (Ar–C); MS *m/z*: 305.2 $C_{14}H_{12}N_2O_6$ (calcd. 304.2); Anal. Calcd: C, 55. 27; H, 3.98; N, 9.21. Found: C, 55.45; H, 4.13; N, 9.43.

H_2L_{IV} (4): brownish (EtOH); yield: 80 %; IR (KBr) ν max 3398, 1613 cm^{-1}; ^1H NMR ($CDCl_3$, 300 MHz,): δ = 9.72 (1H, C_4–OH), 15.40 (1H, C_9–OH), 5.59 (1H, C_5–H), 7.01 (d, J = 8.7 Hz, 1H), 6.93 (s, 1H), 6.85 (d, J = 8.7 Hz, 1H); ^{13}C NMR ($CDCl_3$, 300 MHz): δ = 163.8 (C, C_2), 95.9 (C, C_3), 183.3 (C, C_4), 105.9 (C, C_5), 163.3 (C, C_6), 175.9 (C, C_7), 19.2, 19.9 (C–CH_3), 151.4, 129.2, 125.9, 124.0, 123.7 119.9 (Ar–C); MS *m/z*: 294.2 $C_{14}H_{12}ClNO_4$ (calcd. 293.7); Anal. Calcd: C, 57. 25; H, 4.12; N, 4.77. Found: C, 57.50; H, 4.36; N, 4.98.

*General procedure for the synthesis of organosilicon complexes (**5–16**)*

Disodium salts of the ligands were prepared by stirring the respective ligand (10 mmol) and sodium metal (20 mmol) in 30 mL dry ethanol in an inert dry nitrogen atmosphere. For the synthesis of the complexes, calculated amount of Et_2SiCl_2, Bu_2SiCl_2 or Ph_2SiCl_2 was slowly added to the requisite amount of the disodium salt of the corresponding ligands (Na_2L) in a 1:1 molar ratio in the dry ethanol with

continuous stirring. The mixture was then refluxed for 3–4 h, the precipitated sodium chloride was filtered off, and excess solvent was removed under vacuum. The separated solid was washed with dry *n*-hexane and recrystallized from the mixture of dry ethanol and n-hexane (50:50 v/v) to ensure the purity of the product.

$Et_2Si(L_I)$ (5): dark brown (EtOH); yield: 76 %; IR (KBr) *v* max 1592, 600, 520 cm^{-1}; ^1H NMR ($CDCl_3$, 300 MHz,): $\delta = 5.57$ (1H, C_5–H), 7.56 (d, $J = 8.5$ Hz, 1H), 7.11 (s, 1H), 6.98 (d, $J = 8.5$ Hz, 1H), 1.18 (t, $J = 4.5$ Hz, 6H), 1.01 (q, $J = 4.5$ Hz, 4H), ^{13}C NMR ($CDCl_3$, 300 MHz): $\delta = 163.8$ (C, C_2), 96.8 (C, C_3), 188.1 (C, C_4), 105.3 (C, C_5), 162.7 (C, C_6), 183.0 (C, C_7), 19.8, 19.3 (C–CH_3), 151.0, 128.9, 126.8, 124.5, 121.9 118.5 (Ar–C), $\delta = 9.2$, 11.2 (Si–Et); MS *m/z*: 343.8 $C_{18}H_{22}NO_4Si$ (calcd. 344.4); Anal. Calcd: C, 62.76; H, 6.82; N, 4.15; Si, 8.15. Found: C, 62.42; H, 6.44; N, 4.07; Si, 8.23.

$Bu_2Si(L_I)$ (6): dark brown (EtOH); yield: 74 %; IR (KBr) *v* max 1591, 630, 529 cm^{-1}; ^1H NMR ($CDCl_3$, 300 MHz,): $\delta = 5.58$ (1H, C_5–H), 7.58 (d, $J = 9.1$ Hz, 1H), 7.19 (s, 1H), 7.05 (d, $J = 9.1$ Hz, 1H), 1.53 ($J = 3.2$ Hz, t, 4H), 1.09 ($J = 5.1$ Hz, t, 6H), 0.97–0.91(m, 8H); ^{13}C NMR ($CDCl_3$, 300 MHz): $\delta = 163.9$ (C, C_2), 96.3 (C, C_3), 188.5 (C, C_4), 106.1 (C, C_5), 163.1 (C, C_6), 182.5 (C, C_7), 19.9, 19.2 (C–CH_3), 150.3, 129.6, 127.2, 124.9, 122.7, 118.9 (Ar–C), 13.6, 15.7, 20.5, 21.6 (Si–Bu); MS *m/z*: 401.6 $C_{22}H_{30}NO_4Si$ (calcd. 400.5); Anal. Calcd: C, 65.97; H, 7.55; N, 3.50; Si, 7.01. Found: C, 66.13; H, 7.83; N, 3.58; Si, 6.92.

$Ph_2Si(L_I)$ (7): brown (EtOH); yield: 78 %; IR (KBr) *v* max 1593, 650, 540 cm^{-1}; ^1H NMR ($CDCl_3$, 300 MHz,): $\delta = 5.58$ (1H, C_5–H), 7.64 (d, $J = 7.8$ Hz, 1H), 7.20 (s, 1H), 7.10 (d, $J = 7.8$ Hz, 1H), 7.53–7.46 (m, 4H), 7.30–7.24 (m, 6H); ^{13}C NMR ($CDCl_3$, 300 MHz): $\delta = 163.3$ (C, C_2), 97.7 (C, C_3), 189.3 (C, C_4), 106.5 (C, C_5), 163.3 (C, C_6), 183.8 (C, C_7), 19.6, 19.0 (C–CH_3), 150.8, 130.7, 127.8, 124.7, 123.4, 119.3 (Ar–C), 147.3, 137.5, 133.6, 128.2 (Si–Ph); MS *m/z*: 441.6 $C_{26}H_{22}NO_4Si$ (calcd. 440.5); Anal. Calcd: C, 70.88; H, 5.03; N, 3.18; Si, 6.38. Found: C, 71.03; H, 5.32; N, 2.50; Si, 5.67.

$Et_2Si(L_{II})$ (8): brown (EtOH); yield: 74 %; IR (KBr) *v* max 1599, 656, 556 cm^{-1};^1H NMR ($CDCl_3$, 300 MHz,): $\delta = 5.72$ (1H, C_5–H), 7.20 (d, $J = 8.9$ Hz, 1H), 7.08 (d, $J = 8.9$ Hz, 1H), 6.95 (s, 1H), 1.12 ($J = 4.6$ Hz, t, 6H), 0.98 ($J = 4.6$ Hz, q, 4H); ^{13}C NMR ($CDCl_3$, 300 MHz): $\delta = 163.5$ (C, C_2), 96.9 (C, C_3), 188.9 (C, C_4), 106.1 (C, C_5), 162.3 (C, C_6), 182.0 (C, C_7), 19.9, 19.2 (C–CH_3), 151.9, 127.8, 123.1, 119.2, 118.1 117.5 (Ar–C), 9.1, 10.9 (Si–Et); MS *m/z*: 357.8 $C_{19}H_{24}NO_4Si$ (calcd. 358.4); Anal. Calcd: C, 63.66; H, 6.75; N, 3.91; Si, 7.83. Found: C, 63.92; H, 6.53; N, 3.40; Si, 7.70.

$Bu_2Si(L_{II})$ (9): brown (EtOH); yield: 77 %; IR (KBr) *v* max 1600, 639, 560 cm^{-1}; ^1H NMR ($CDCl_3$, 300 MHz,): $\delta = 5.71$ (1H, C_5–H), 7.25 (d, $J = 9.3$ Hz, 1H), 7.18 (d, $J = 9.3$ Hz, 1H), 7.05 (s, 1H), 1.50 (t, $J = 2.3$ Hz, 4H), 0.99 (t, $J = 4.3$ Hz, 6H), 0.95–0.90 (m, 8H); ^{13}C NMR ($CDCl_3$, 300 MHz): $\delta = 163.8$ (C, C_2), $\delta = 96.7$ (C, C_3), 188.5 (C, C_4), 105.9 (C, C_5), 162.0 (C, C_6), 181.9 (C, C_7), 19.5, 19.1 (C–CH_3), 149.4, 126.9, 121.7, 118.9, 117.6, 117.2 (Ar–C), 13.3, 15.3, 20.6, 21.5 (Si–Bu); MS *m/z*: 414.9 $C_{23}H_{32}NO_4Si$ (calcd. 414.5); Anal. Calcd: C, 66.63; H, 7.78; N, 3.38; Si, 6.77. Found: C, 66.95; H, 7.43; N, 3.26; Si, 6.66.

$Ph_2Si(L_{II})$ (10): dark brown (EtOH): yield: 72 %; IR (KBr) *v* max 1603, 636, 558 cm^{-1}; ^1H NMR ($CDCl_3$, 300 MHz,): $\delta = 5.73$ (1H, C_5–H), 7.61 (d, $J = 8.8$ Hz, 1H), 7.01 (d, $J = 8.8$ Hz, 1H), 7.13 (s, 1H), 7.45–7.33 (m, 4H), 7.29–7.14 (m, 6H); ^{13}C NMR ($CDCl_3$, 300 MHz): $\delta = 163.9$ (C, C_2), 96.4 (C, C_3), 189.8 (C, C_4), 106.8 (C, C_5), 162.5 (C, C_6), 182.7 (C, C_7), 18.8, 18.6 (C–CH_3), 150.1, 127.4, 122.6, 118.5, 117.8, 117.1 (Ar–C), 148.8, 138.1, 130.9, 121.8 (Si–Ph); MS *m/z*: 453.9 $C_{27}H_{24}NO_4Si$ (calcd. 454.5); Anal. Calcd: C, 71.34; H, 5.32; N, 3.08; Si, 6.18. Found: C, 71.62; H, 5.61; N, 3.16; Si, 5.45.

$Et_2Si(L_{III})$ (11): dark brown (EtOH); yield: 73 %; IR (KBr) *v* max 1600, 636, 548 cm^{-1}; ^1H NMR ($CDCl_3$, 300 MHz,): $\delta = 5.80$ (1H, C_5–H), 7.55 (d, $J = 8.0$ Hz, 1H), 7.13 (s, 1H), 7.11 (d, $J = 8.0$ Hz, 1H), 1.17 ($J = 2.9$, t, 6H), 0.99 (q, $J = 2.9$, 4H); ^{13}C NMR ($CDCl_3$, 300 MHz): $\delta = 163.9$ (C, C_2), 96.8 (C, C_3), 188.7 (C, C_4), 107.0 (C, C_5), 162.8 (C, C_6), 183.7 (C, C_7), 19.9, 19.4 (C–CH_3), 150.3, 128.7, 128.0, 124.5, 122.7, 119.4 (Ar–C), 9.3, 11.1 (Si–Et); MS *m/z*: 390.1 $C_{18}H_{21}N_2O_6Si$ (calcd. 389.4); Anal. Calcd: C, 55.51; H, 5.43; N, 7.19; Si, 7.21. Found: C, 55.83; H, 5.89; N, 7.08; Si, 6.94.

$Bu_2Si(L_{III})$ (12): dark brown (EtOH); yield: 74 %; IR (KBr) *v* max 1599, 647, 538 cm^{-1}; ^1H NMR ($CDCl_3$, 300 MHz,): $\delta = 5.81$ (1H, C_5–H), 7.56 (d, $J = 8.9$ Hz, 1H), 7.18 (s, 1H), 6.99 (d, $J = 8.9$ Hz, 1H), 1.60 (t, $J = 4.1$ Hz, 4H), 1.19 (t, $J = 3.8$ Hz, 6H), 0.98–0.92 (m, 8H); ^{13}C NMR ($CDCl_3$, 300 MHz): $\delta = 163.7$ (C, C_2), 96.5 (C, C_3), 189.6 (C, C_4), 106.9 (C, C_5), 162.6 (C, C_6), 184.2 (C, C_7), 20.1, 19.6 (C–CH_3), 152.1, 129.2, 128.7, 125.1, 123.1, 119.6 (Ar–C), 14.1, 15.0, 20.2, 21.9 (Si–Bu); MS *m/z*: 445.9 $C_{22}H_{29}NO_6Si$ (calcd. 445.0); Anal. Calcd: C, 59.30; H, 6.56; N, 6.29; Si, 6.30. Found: C, 59.63; H, 6.82; N, 6.15; Si, 5.83.

$Ph_2Si(L_{III})$ (13): brown (EtOH); yield: 76 %; IR (KBr) *v* max 1601, 650, 528 cm^{-1}; ^1H NMR ($CDCl_3$, 300 MHz,): $\delta = 5.82$ (1H, C_5–H), 7.67 (d, $J = 9.0$ Hz, 1H), 7.21 (s, 1H), 7.19 (d, $J = 9.0$ Hz, 1H), 7.56–7.46 (m, 4H), 7.27–7.22 (m, 6H); ^{13}C NMR ($CDCl_3$, 300 MHz): $\delta = 163.8$ (C, C_2), 96.9 (C, C_3), 190.1 (C, C_4), 107.2 (C, C_5), 162.8 (C, C_6), 184.9 (C,C_7), 20.4, 19.5 (C–CH_3), 151.9, 129.6, 128.9, 125.2, 123.4, 119.9 (Ar–C), 149.5, 139.7, 133.2, 130.6 (Si–Ph); MS *m/z*: 485.9 $C_{26}H_{21}NO_6Si$

(calcd. 485.5); Anal. Calcd: C, 64.32; H, 4.36; N, 5.77; Si, 5.78. Found: C, 64.63; H, 4.65; N, 5.71; Si, 5.25.

$Et_2Si(L_{IV})$ (14): dark brown (EtOH); yield: 68 %; IR (KBr) ν max 1593, 630, 560 cm^{-1}; ^1H NMR ($CDCl_3$, 300 MHz,): $\delta = 5.57$ (1H, C_5–H), 7.51 (d, $J = 8.3$ Hz, 1H), 6.99 (d, $J = 8.3$ Hz, 1H), 7.23 (s, 1H), 1.19 (t, $J = 3.1$ Hz, 6H), 1.08 (q, $J = 2.6$ Hz, 4H); ^{13}C NMR ($CDCl_3$, 300 MHz): $\delta = 164.0$ (C, C_2), 96.7 (C, C_3), 190.5 (C, C_4), 106.2 (C, C_5), 163.8 (C, C_6), 185.6 (C, C_7), 19.9, 19.3 (C, C–CH_3), 151.9, 129.7, 126.2, 124.3, 123.8 120.2 (Ar–C), 9.5, 11.6 (Si-Et); MS *m/z*: 378.3 $C_{18}H_{21}ClNO_4Si$ (calcd. 378.9); Anal. Calcd: C, 57.06; H, 5.59; N, 3.70; Si, 7.41. Found: C, 57.32; H, 5.82; N, 3.67; Si, 6.66.

$Bu_2Si(L_{IV})$ (15): dark brown (EtOH); yield: 73 %; IR (KBr) ν max 1598, 626, 550 cm^{-1}; ^1H NMR ($CDCl_3$, 300 MHz,): $\delta = 5.58$ (1H, C_5–H), 7.58 (d, $J = 8.2$ Hz, 1H), 7.19 (s, 1H), 7.17 (d, $J = 8.2$ Hz, 1H), 1.65 (t, $J = 3.4$, 4H), 1.21 (t, $J = 4.1$, 6H), 0.97–0.92 (m, 8H); ^{13}C NMR ($CDCl_3$, 300 MHz): $\delta = 163.7$ (C, C_2), 96.5 (C, C_3), 191.3 (C, C_4), 106.5 (C, C_5), 164.1 (C, C_6), 186.2 (C, C_7), 19.7, 19.1 (C–CH_3), 152.2, 130.3, 126.5, 124.7, 124.3 120.2 (Ar–C), 4.5, 15.9, 20.7, 21.3 (Si–Bu); MS *m/z*: 435.8 $C_{22}H_{29}ClNO_4Si$ (calcd. 435.0); Anal. Calcd: C, 60.74; H, 6.72; N, 3.22; Si, 6.46. Found: C, 60.96; H, 6.93; N, 3.28; Si, 5.96.1

$Ph_2Si(L_{IV})$ (16): brown (EtOH); yield: 76 %; IR (KBr) ν max 1595, 639, 560 cm^{-1}; ^1H NMR ($CDCl_3$, 300 MHz,): $\delta = 5.60$ (1H, C_5–H), 7.61 (d, $J = 7.9$ Hz, 1H), 7.25 (s, 1H), 7.18 (d, $J = 7.9$ Hz, 1H), 7.66–7.65 (m, 4H), 7.39–7.31 (m, 6H); ^{13}C NMR ($CDCl_3$, 300 MHz): $\delta = 163.9$ (C, C_2), 96.8 (C, C_3), 191.7 (C, C_4), 106.8 (C, C_5), 164.3 (C, C_6), 186.5 (C, C_7), 20.2, 19.5 (C–CH_3), 152.5, 130.7, 126.8, 125.2, 124.6 120.7 (Ar–C), 149.9, 139.7, 134.2, 131.8 (Si–Ph); MS *m/z*: 474.2 $C_{26}H_{21}ClNO_4Si$ (calcd. 474.9); Anal. Calcd: C, 65.74; H, 4.46; N, 2.95; Si, 5.91. Found: C, 65.45; H, 4.71; N, 2.83; Si, 5.35.

Antimicrobial activity

For determination of in vitro antimicrobial activity, the ligands and their organosilicon complexes were screened against Gram-positive bacteria viz. *Bacillus subtilis* (MTCC no. 2063) and *Staphylococcus aureus* (MTCC no. 2901) and the Gram-negative bacteria viz. *Escherichia coli* (MTCC no. 1652), as well as in vitro antifungal activity against *Candida albicans* (MTCC no. 183) and *Aspergillus niger* (MTCC no. 1344), using two fold serial dilution technique in double-strength nutrient broth and Sabouraud dextrose broth, respectively (Cappucino and Sherman, 1999). The incubation period of *A. niger* and *C. albicans* was 7 days at 25 ± 1 °C and 48 h at 37 ± 1 °C, respectively, whereas for bacteria it was 24 h at 37 ± 1 °C. Stock solutions were prepared by dissolving the compounds in dry DMSO with concentration of 100 μg/mL. Norfloxacin and fluconazole were used as standards for comparing the activity of **1–16** compounds. Each sample was assayed in triplicate and the mean values were calculated.

QSAR studies

Pre-optimization of structure of (**1–16**) was done with the Molecular Mechanics Force Field (MM^+) procedure included in Hyperchem 6.03 (1993) and the consequential geometries were further refined by means of the semiempirical method PM3 (Parametric Method-3). A gradient norm limit of 0.01 kcal/Å was chosen for the geometry optimization. To calculate physicochemical properties, lowest energy structure was used for each molecule using TSAR 3.3 (2000) software for Windows. Further, the regression analysis was performed using the SPSS (1999) software package.

Results and discussion

Chemistry

The ligands and their organosilicon complexes were synthesized using the synthetic procedure described in Scheme 1. The ligands (**1–4**) were prepared by the condensation of dehydroacetic acid and *p*-substituted 2-aminophenol. The homogeneity of the compounds was regularly monitored through TLC. Dichlorodiorganosilane was reacted with the disodium salt of the Schiff base in dry ethanol in 1:1 molar ratio. The elemental analyses data of the compounds **1–16** are well in agreement with the corresponding molecular formulae with small deviation from actual values for each element. The low molar conductance values for the complexes in the range of 8.0–12.0 Ω^{-1} cm^2 mol^{-1} in dry dimethyl sulfoxide indicate the non-electrolytic nature of complexes. Single crystals of the complexes could not be obtained as powdery substance got precipitated from the solution upon each attempt of crystallization.

Spectral studies

All the synthesized compounds were well characterized by IR, NMR (^1H, ^{13}C and ^{29}Si) and mass spectral studies in addition to elemental analyses which were in full agreement with their molecular structures. The infrared spectra recorded using KBr pellets of the complexes were compared with that of the Schiff base ligands to ascertain the coordination sites of the ligand on the basis of shifts in the frequency of various groups and the absence of certain absorptions, which may be due to changes in the electronic

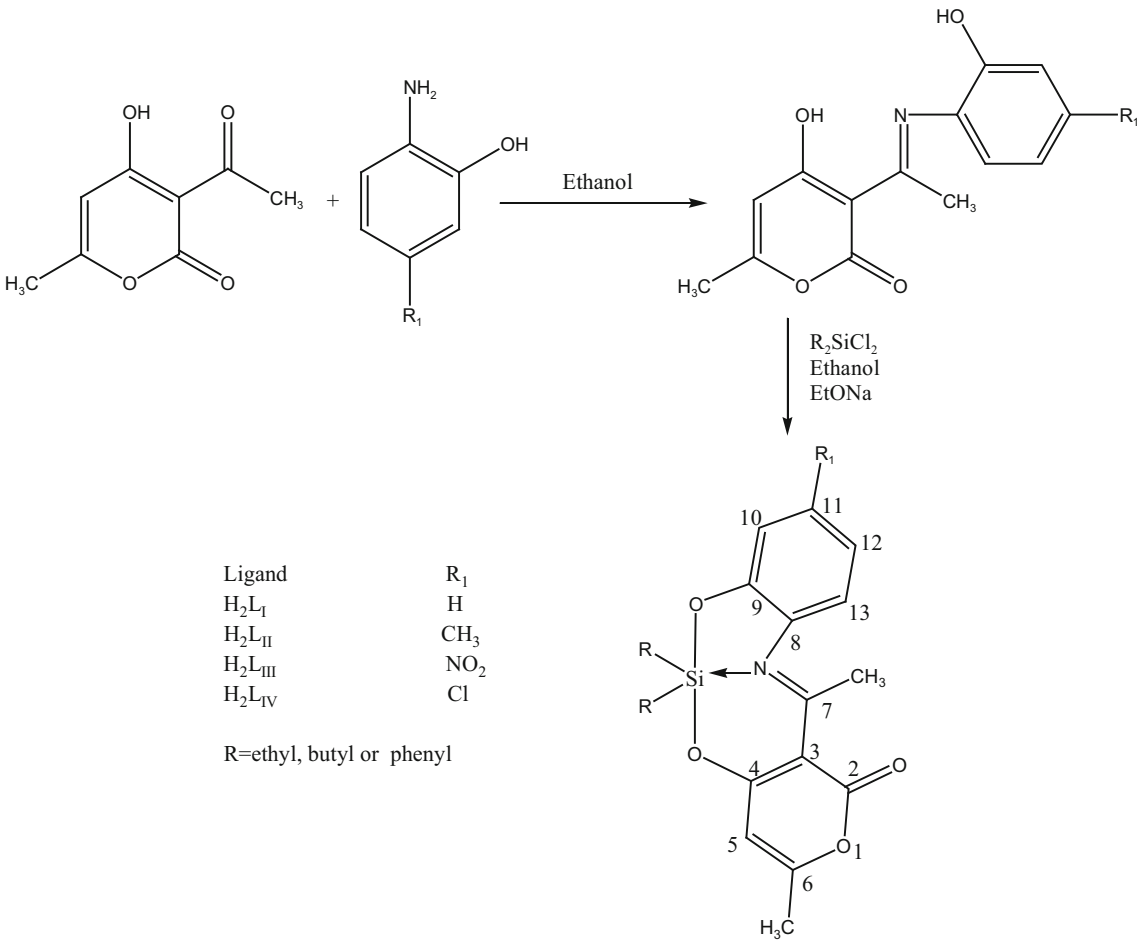

Scheme 1 Synthesis of Schiff base ligands and their organosilicon complexes

environment of the ligands after the formation of silicon ligand bond. In the spectra of the ligands, a broad band centre at 3380–3398 cm^{-1} was due to ν(OH), and the broadness of this band suggested the presence of a hydrogen bond between the OH group and the azomethine nitrogen of the ligand. In addition, a weak band in the region 2780–2800 cm^{-1} was attributed to an intramolecular hydrogen bond due to an OH group. The absorption band due to ν(OH) was found to be completely absent in the complexes, thereby suggesting the involvement of both phenolic hydroxyl groups after deprotonation in coordination. Moreover, the phenolic ν(C–O) stretching and bending vibrations, at 1500–1520 and 1270–1290 cm^{-1}, respectively, as expected for an uncoordinated phenol were found to be shifted to higher frequencies by 20–30 cm^{-1}. Coordination of the oxygen to the silicon atom was further confirmed by the appearance of bands in the region of 520–560 cm^{-1} which were assigned to ν(Si–O). The shift in the absorption bands due to ν(C=N) which earlier appeared at 1605–1620 cm^{-1} in the ligands to a lower frequencies by 10–20 cm^{-1} in the complexes indicated that coordination indeed had taken place through the nitrogen atom (Nejo *et al.*, 2010). New bands also appeared in the range of 600–650 cm^{-1} which were assigned to ν(Si–N).

The ^{1}H, ^{13}C and ^{29}Si NMR spectra of the ligands and their corresponding organosilicon(IV) complexes were recorded in $CDCl_3$ using TMS as the internal standard. ^{1}H NMR spectra of the free ligands have broad singlets at δ 8.35 ppm and δ 15.0 ppm due to the OH protons attached to C_4 and C_9, respectively, which completely disappeared from the spectra of the corresponding complexes indicating deprotonation with the formation of the covalent bond between the oxygen and silicon atom. Sharp singlets at δ 5.70 ppm and δ 2.54 ppm due to the CH proton and methyl protons attached to carbon C_6 of the pyran-2-one ring remained almost unchanged on complexation, while a downfield shift of δ ~0.1 was observed in the methyl protons attached to C_7 which appeared as a singlet. Aromatic protons appeared as a singlet and a doublet at δ 6.85, and δ 6.96–7.10 ppm, respectively, and shifted slightly downfield in the complexes. A new triplet at δ 0.9 ppm and a quartet at δ 1.1 ppm due to the ethyl protons attached to

the silicon atom or a multiplet at δ 7.1–7.4 ppm due to the phenyl group attached to the silicon atom appeared in the spectra of the complexes. A singlet and a multiplet at δ 1.5 ppm and δ 0.9 ppm were assigned to the n-butyl group attached to the silicon atom.

In the ^{13}C NMR spectra of the ligands, the signal at δ 175.5 ppm due to the azomethine carbon was shifted towards a lower value by δ 10–15 ppm in the complexes. This observed downfield change in chemical shift indicates the coordination of the azomethine nitrogen to the silicon atom upon the complexation. Signals due to C_4 and C_9 were shifted towards a higher chemical shift value in the organosilicon complexes. The signal for the methyl carbon appeared at δ 19.1–19.8 ppm in the spectra of the ligands and remained almost same in the complexes. The signal due to the carbons of the ethyl and *n*-butyl groups attached to the silicon atom appeared in the range of δ 9.1–12.9 ppm and δ 13.3–26.5 ppm. The resonances due to the carbons of phenyl ring attached to the silicon atom appeared in the range of δ 128.8–148.8 ppm. The signals for the aromatic carbons appeared in the range of δ 117.6–126.8 ppm. Shifts in the positions of other carbon atoms involved in complex formation indicate a bonding pattern in the complexes.

The pentacoordinated silicon atom in all the complexes showed a sharp singlet at δ −95.6 to −110.9 ppm in the ^{29}Si NMR spectra of the complexes. On the basis of above spectral data, it may be concluded that the complexes are five-coordinated and probably possess trigonal bipyramidal geometry around silicon atom.

LC-MS of the ligands and their corresponding organosilicon complexes were recorded and the mass spectrum of H_2L_{II} (**2**) showed a well-defined molecular ion peak at $m/z = 274.4$ The corresponding silicon complex $Et_2Si(L_{II})$ showed a base peak at $m/z = 357.8$. The molecular ion peaks in spectra of the other ligands and their organosilicon complexes are summarized in experimental part.

Antimicrobial activity

All the newly synthesized compounds were subjected to in vitro antibacterial activity against the Gram-positive bacteria viz. *B. subtilis* and *S. aureus* and the Gram-negative bacteria viz. *E. coli*, as well as in vitro antifungal activity against *C. albicans* and *A. niger*. Minimum inhibitory concentrations (MICs) were determined by means of twofold serial dilution technique. As evident from antimicrobial activity output, most of the compounds exhibited excellent activity. Results indicated clear concentration-dependent activity, as growth of bacteria and fungus decreases with increase in concentration of the tested compounds. Norfloxacin and fluconazole were used as standard drugs (positive control) for antibacterial and antifungal activity, respectively, whereas DMSO was used as the negative control which produces no visible effect on activity.

Studies have shown that the nitrogen of azomethine group with lone pair of electron has considerable biological importance (Dholakiya and Patel, 2004). The activity of the ligands therefore may be reorganized due to the presence of >C=N group. The ligands H_2L_{III} (**3**) and H_2L_{IV} (**4**), having nitro- and chloro-substituted phenyl groups, showed better activity towards all microorganisms than the ligand H_2L_{II} (**2**) with a methyl substituted phenyl group. Organosilicon complexes were more active towards the bacteria and fungi than their corresponding ligands under identical experimental conditions. This increase in the activity on complexation is explained on the basis of chelation theory (Devi and Batra, 2015). According to this theory, when biological active molecule is attached to the silicon atom, the lipophilic nature is increased which favours their permeation through lipid layer of the cell membrane of microorganisms, thus interfering the cell process which further restrict the growth of organism. None of the compounds showed better inhibition than the conventional fungicides and bactericides used. Among all the complexes $Ph_2Si(L_{I–IV})$ [**7**, **10**, **13**, **16**] were found to be more potent than $Bu_2Si(L_{I–IV})$ or $Et_2Si(L_{I–IV})$ which is in agreement with our previous work (Devi *et al.*, 2012b, c).

QSAR studies

In order to understand the experimental antimicrobial data on theoretical basis, quantitative structure activity relationship (QSAR) studies were undertaken between in vitro antimicrobial activity of synthesized compounds and descriptors coding for lipophilic, electronic, steric and topological properties of the molecules being discussed, using the linear free energy relationship (LFER) model (Hansch and Fujita, 1964). Data set of all **1–16** was used for the regression analysis, and no outlier was found. The standard drugs were not included in the model development as they belong to a different structural series.

The biological activity data determined as MIC values were first transformed into pMIC values (i.e. –log MIC) and used as dependent variables in QSAR study (Table 1). Molecular descriptors (independent variables) like log of octanol–water partition coefficient (log *P*), molar refractivity (MR), Kier's molecular connectivity ($^0\chi$, $^0\chi^v$, $^1\chi$, $^1\chi^v$, $^2\chi$, $^2\chi^v$) and shape (κ_1, $\kappa\alpha_1$, $\kappa\alpha_2$, $\kappa\alpha_3$) topological indices, Randic topological index (*R*), Balaban topological index (*J*), Wiener topological index (*W*), total energy (T_e), energies of highest occupied molecular orbital (HOMO) and lowest unoccupied molecular orbital (LUMO), dipole moment (μ) and electronic energy (E_e) (Hansch *et al.*,

Table 1 Antimicrobial activity (pMIC)

S. No.	Ligand/complexes	$pMIC_{sa}$	$pMIC_{bs}$	$pMIC_{ec}$	$pMIC_{an}$	$pMIC_{ca}$	$pMIC_{ab}$	$pMIC_{af}$	$pMIC_{am}$
1	H_2L_I	0.41	0.41	0.41	0.71	0.41	0.41	0.56	0.47
2	H_2L_{II}	0.44	0.44	0.44	0.44	0.44	0.44	0.44	0.44
3	H_2L_{III}	0.48	0.48	0.78	0.48	0.78	0.58	0.63	0.60
4	H_2L_{IV}	0.47	0.77	0.47	0.77	0.47	0.57	0.62	0.59
5	$Et_2Si(L_I)$	1.14	1.44	1.14	1.44	1.44	1.24	1.44	1.32
6	$Bu_2Si(L_I)$	1.51	1.20	1.20	1.51	1.81	1.30	1.66	1.44
7	$Ph_2Si(L_I)$	1.85	1.25	1.55	1.85	1.25	1.55	1.55	1.55
8	$Et_2Si(L_{II})$	1.46	1.46	1.15	1.15	1.76	1.36	1.46	1.40
9	$Bu_2Si(L_{II})$	1.22	1.22	1.22	1.52	1.52	1.22	1.52	1.34
10	$Ph_2Si(L_{II})$	1.56	1.56	1.86	1.86	1.56	1.66	1.71	1.68
11	$Et_2Si(L_{III})$	1.19	1.79	1.49	1.19	1.19	1.49	1.19	1.37
12	$Bu_2Si(L_{III})$	1.25	1.55	1.25	1.55	1.85	1.35	1.70	1.49
13	$Ph_2Si(L_{III})$	1.59	1.29	1.59	1.29	2.19	1.49	1.74	1.59
14	$Et_2Si(L_{IV})$	1.48	1.48	1.76	1.78	1.48	1.58	1.63	1.60
15	$Bu_2Si(L_{IV})$	1.24	1.24	1.84	1.54	1.84	1.44	1.69	1.54
16	$Ph_2Si(L_{IV})$	1.58	1.58	1.58	2.18	1.88	1.58	2.03	1.76
Tetracyclin		>2.15	>2.15	>2.15	–	–	>2.15	–	
Chloramphenicol		>2.01	>2.01	>2.01	–	–	>2.01	–	–
Cycloheximide		–	–	–	>1.95	>1.95	–	>1.95	–
Fluconazole		–	–	–	>1.99	>1.99	–	>1.99	–

1973; Kier and Hall, 1976; Randic, 1975; Balaban, 1982; Randic, 1993), were calculated for synthesized ligands and their complexes and used as independent variables. Values of selected molecular descriptors are presented in Table 2.

Since multi-target QSAR (mt-QSAR) models are better in describing the antimicrobial activity, and therefore in order to develop mt-QSAR models, initially we calculated the average antibacterial, antifungal and antimicrobial

Table 2 Values of selected molecular descriptors used in QSAR study

S. No.	MR	$^1\chi$	$^1\chi^v$	$^3\chi$	$^3\chi^v$	κ_1	W	LUMO	HOMO	μ
1	71.66	8.99	5.66	1.51	0.53	15.39	708.00	−0.88	−8.60	4.97
2	76.70	9.38	6.07	1.80	0.69	16.37	814.00	−0.87	−8.46	4.56
3	78.99	10.29	6.16	2.01	0.64	18.34	1068.00	−1.19	−9.29	10.90
4	76.47	9.38	6.17	1.80	0.73	16.37	814.00	−0.97	−8.67	6.29
5	9.31	11.48	10.56	2.08	1.53	18.78	1132.00	−0.86	−8.52	2.55
6	11.17	13.48	12.56	2.08	1.53	22.68	1766.00	−0.86	−8.51	2.64
7	12.48	15.57	12.32	2.18	1.63	23.73	2368.00	−0.76	−8.70	8.03
8	9.78	11.87	10.97	2.37	1.70	19.75	1273.00	−0.84	−8.43	2.42
9	11.63	13.87	12.97	2.37	1.70	23.66	1941.00	−0.85	−8.43	2.53
10	12.95	15.96	12.73	2.47	1.80	24.68	2573.00	−0.82	−8.40	7.56
11	12.95	12.78	11.06	2.58	1.65	21.70	1607.00	−1.50	−9.08	7.79
12	12.95	14.78	13.06	2.58	1.65	25.62	2351.00	−1.50	−9.07	7.82
13	13.09	16.87	12.82	2.68	1.74	26.60	3051.00	−1.44	−9.03	7.83
14	9.81	11.87	11.07	2.37	1.73	19.75	1273.00	−0.99	−8.62	3.25
15	11.66	13.87	13.07	2.37	1.73	23.66	1941.00	−0.99	−8.61	3.36
16	12.97	15.96	12.82	2.47	1.83	24.68	2573.00	−0.83	−8.75	8.01

Table 3 Correlation matrix for antibacterial activity

	$pMIC_{ab}$	MR	$^{1}\chi$	$^{1}\chi^{v}$	$^{3}\chi$	$^{3}\chi^{v}$	κ_1	W	LUMO	HOMO	μ
$pMIC_{ab}$	1.000										
MR	−0.945	1.000									
$^{1}\chi$	0.842	−0.762	1.000								
$^{1}\chi^{v}$	0.927	−0.946	0.894	1.000							
$^{3}\chi$	0.860	−0.791	0.815	0.837	1.000						
$^{3}\chi^{v}$	0.974	−0.975	0.827	0.962	0.873	1.000					
κ_1	0.813	−0.760	0.975	0.913	0.856	0.822	1.000				
W	0.760	−0.665	0.987	0.830	0.788	0.745	0.968	1.000			
LUMO	−0.091	0.046	−0.159	−0.090	−0.463	−0.069	−0.282	−0.231	1.000		
HOMO	0.042	−0.164	−0.107	0.085	−0.267	0.127	−0.183	−0.181	0.821	1.000	
μ	−0.033	0.273	0.248	−0.126	0.177	−0.170	0.224	0.336	−0.474	−0.771	1.000

activity values of dehydroacetic acid-derived Schiff base ligands and their organosilicon(IV) complexes which are presented in Table 1. The correlation matrix for antibacterial activity is presented in Table 3. In general, high colinearity ($r > 0.5$) was observed between different parameters. The high interrelationship was observed between topological parameters, such as first-order molecular connectivity index ($^{1}\chi$) and Wiener index (W) ($r = 0.987$), and low interrelationship was observed for electronic parameter, energy of lowest unoccupied molecular orbital (LUMO) and molar refractivity (MR) ($r = 0.046$). Correlation of antibacterial, antifungal and antimicrobial activities of **1–16** compounds with their molecular descriptors is given in Table 4.

Correlation matrix (Table 3) indicated that valence third-order molecular connectivity index ($^{3}\chi^{v}$) was the most dominating descriptor in describing the antibacterial activity of synthesized ligands and their complexes. So, QSAR model for antibacterial activity (Eq. 1) was developed using $^{3}\chi^{v}$.

LR-mt-QSAR model for antibacterial activity

$$pMIC_{ab} = 0.905\,^{3}\chi^{v} - 0.086 \quad (1)$$

$$n = 16 \quad r = 0.974 \quad q^2 = 0.936 \quad s = 0.103 \quad F = 259.85$$

Here and thereafter, n—number of data points, r—correlation coefficient, q^2—cross-validated r^2 obtained by leave one out method, s—standard error of the estimate and F—Fischer statistics.

The coefficient of third-order molecular connectivity index ($^{3}\chi^{v}$) was found to be high in QSAR model developed to describe the antibacterial activity (1), which indicated that there is a positive correlation between $^{3}\chi^{v}$ and antibacterial activity of the compounds which means that antibacterial activity values of synthesized compounds will increase with increase in their $^{3}\chi^{v}$ values and vice versa. The organosilicon complexes $Ph_2Si(L_{I–IV})$ have highest $^{3}\chi^{v}$ values (1.63, 1.80, 1.74 and 1.83, Table 2) for ligands L_I,

Table 4 Correlation of antibacterial, antifungal and antimicrobial activity of the synthesized compounds with calculated molecular descriptors

Descriptors	$pMIC_{ab}$	$pMIC_{af}$	$pMIC_{am}$
Cos E	0.563	0.605	0.591
MR	−0.945	−0.927	−0.953
$^{0}\chi$	0.841	0.872	0.869
$^{0}\chi^{v}$	0.911	0.952	0.945
$^{1}\chi$	0.842	0.873	0.870
$^{1}\chi^{v}$	0.927	0.960	0.957
$^{2}\chi$	0.836	0.853	0.858
$^{2}\chi^{v}$	0.951	0.957	0.970
$^{3}\chi$	0.860	0.800	0.849
$^{3}\chi^{v}$	0.974	0.949	0.980
κ_1	0.813	0.862	0.848
κ_2	0.730	0.821	0.782
κ_3	0.509	0.644	0.577
$\kappa\alpha_1$	0.836	0.894	0.876
$\kappa\alpha_2$	0.751	0.853	0.808
$\kappa\alpha_3$	0.531	0.668	0.600
R	0.842	0.873	0.870
J	−0.642	−0.591	−0.631
W	0.760	0.806	0.794
T_e	−0.808	−0.832	−0.832
E_e	−0.852	−0.893	−0.884
N_e	0.853	0.896	0.887
SA	0.846	0.915	0.891
IP	−0.042	−0.092	−0.064
LUMO	−0.091	−0.015	−0.059
HOMO	0.042	0.092	0.064
μ	−0.033	−0.111	−0.067

Table 5 Observed, predicted and residual antimicrobial activities

Comp.	$pMIC_{ab}$			$pMIC_{af}$			$pMIC_{am}$		
	Obs.	Pre.	Res.	Obs.	Pre.	Res.	Obs.	Pre.	Res.
1	0.41	0.39	0.02	0.56	0.52	0.05	0.47	0.41	0.06
2	0.44	0.54	−0.11	0.44	0.59	−0.15	0.44	0.57	−0.13
3	0.58	0.49	0.09	0.63	0.60	0.03	0.60	0.52	0.09
4	0.57	0.57	0.00	0.62	0.60	0.02	0.59	0.60	−0.01
5	1.24	1.30	−0.06	1.44	1.34	0.10	1.32	1.36	−0.05
6	1.30	1.30	0.00	1.66	1.68	−0.02	1.44	1.36	0.08
7	1.55	1.39	0.16	1.55	1.64	−0.09	1.55	1.45	0.09
8	1.36	1.45	−0.10	1.46	1.41	0.05	1.40	1.52	−0.13
9	1.22	1.45	−0.23	1.52	1.75	−0.23	1.34	1.52	−0.18
10	1.66	1.54	0.12	1.71	1.70	0.01	1.68	1.61	0.07
11	1.49	1.40	0.09	1.19	1.42	−0.23	1.37	1.47	−0.10
12	1.35	1.40	−0.05	1.70	1.76	−0.06	1.49	1.47	0.02
13	1.49	1.49	0.00	1.74	1.72	0.02	1.59	1.56	0.03
14	1.58	1.48	0.09	1.63	1.43	0.20	1.60	1.55	0.04
15	1.44	1.48	−0.04	1.69	1.76	−0.07	1.54	1.55	−0.01
16	1.58	1.57	0.01	2.03	1.72	0.31	1.76	1.64	0.12

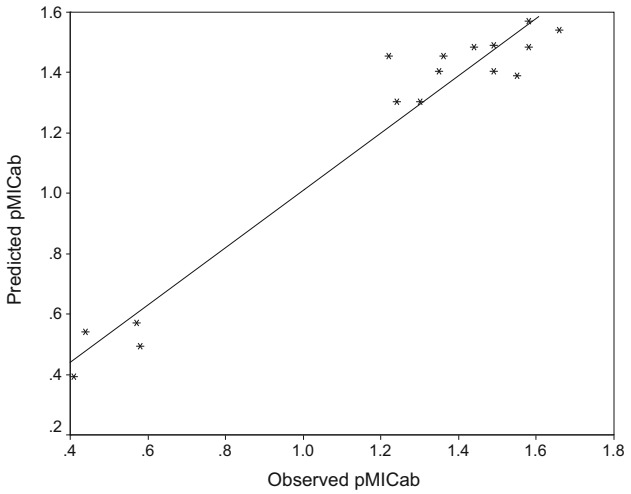

Fig. 1 Plot of observed $pMIC_{ab}$ against predicted $pMIC_{ab}$ by Eq. 1

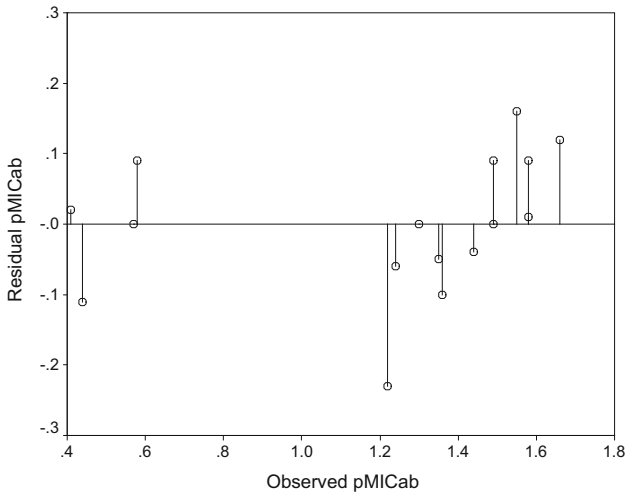

Fig. 2 Plot of observed $pMIC_{ab}$ against residual $pMIC_{ab}$ by Eq. 1

L_{II}, L_{III} and L_{IV}, respectively, as compared to their counterparts $Bu_2Si(L_{I–IV})$ and $Et_2Si(L_{I–IV})$, thereby indicating $Ph_2Si(L_{I–IV})$ [**7**, **10**, **13**, **16**] complexes have better antibacterial activity.

The developed QSAR model (1) was cross-validated by $q^2 = 0.936$ obtained by leave one out (LOO) method. The value of q^2 higher than 0.5 indicated that the model developed is a valid one also justified by closeness of observed and predicted values (Table 5), the mt-QSAR model for antibacterial activity given by (1) is a valid one (Golbraikh and Tropsha, 2002). Developed model for antibacterial activity expressed by this equation is also favoured by the plot of predicted $pMIC_{ab}$ against observed $pMIC_{ab}$ (Fig. 1). Further, the plot of observed $pMIC_{ab}$ versus residual $pMIC_{ab}$ (Fig. 2) indicated that there was no systemic error in model development as the propagation of error was observed on both sides of zero (Kumar *et al.*, 2007).

Topological parameter, valence first-order molecular connectivity index ($^1\chi^v$), was found to be the dominating descriptor for the antifungal activity of **1–16** (Table 4).

LR-mt-QSAR model for antifungal activity

$$\mathrm{pMIC_{af}} = 0.168\,{}^{1}\chi^{v} - 0.434 \quad (2)$$

$$n = 16 \quad r = 0.960 \quad q^2 = 0.902 \quad s = 0.146 \quad F = 164.12$$

As in case of antibacterial activity, antifungal activity of **1**–**16** is also positively correlated with their ${}^{1}\chi^{v}$ values which means that the antifungal activity of **1**–**16** will increase with increase in their ${}^{1}\chi^{v}$ values (Tables 2 and 3).

QSAR model for antifungal activity, i.e. Equation (2) was cross-validated by q^2 value ($q^2 = 0.902$) obtained by leave one out (LOO) method. Further, as the observed and predicted values are close to each other (Table 5), the mt-QSAR model for antifungal activity (Eq. 2) is a valid one (Golbraikh and Tropsha, 2002).

Topological parameter valence third-order molecular connectivity index (${}^{3}\chi^{v}$) was found to be most effective in describing antimicrobial activity of the synthesized compounds (Table 4).

LR-mt-QSAR model for antimicrobial activity

$$\mathrm{pMIC_{am}} = 0.946\,{}^{3}\chi^{v} - 0.0871 \quad (3)$$

$$n = 16 \quad r = 0.980 \quad q^2 = 0.948 \quad s = 0.094 \quad F = 338.52$$

Antimicrobial activity of **1**–**16** is positively correlated with valence third-order molecular connectivity index (${}^{3}\chi^{v}$) which means that antimicrobial activity of the synthesized compounds will increase with increase in their ${}^{3}\chi^{v}$ values (Tables 1, 2). The molecular connectivity index, and adjacency-based topological index proposed by Randic, is denoted by χ and is defined as sum over all the edges (ij) as per following

$$\chi = \sum_{i}^{n} \left(V_i V_j\right)^{-1/2} \quad i = 1$$

where V_i and V_j are the degrees of adjacent vertices i and j, and n is the number of vertices in a hydrogen suppressed molecular structure (Lather and Madan, 2005). The topological index χ signifies the degree of branching, connectivity of atoms and unsaturation in the molecule, which accounts for variation in activity (Mahiwal *et al.*, 2012).

High value of q^2 (0.948) as well as the low residual values (Table 5) favoured the validity of QSAR model for antimicrobial activity (3). Developed model expressed by Eq. 3 also favoured by plot of predicted $\mathrm{pMIC_{am}}$ against observed $\mathrm{pMIC_{am}}$ (Fig. 3). The plot of observed $\mathrm{pMIC_{am}}$ vs residual $\mathrm{pMIC_{am}}$ (Fig. 4) indicated that there was no systemic error in model development as the propagation of error was observed on both sides of zero (Kumar *et al.*, 2007).

It was observed from the mt-QSAR models [Eq. 1–3] that the antibacterial, antifungal and the overall antimicrobial activities of **1**–**16** were governed by topological parameters, valence first- and third-order molecular connectivity indices (${}^{1}\chi^{v}$ and ${}^{3}\chi^{v}$).

Generally for QSAR studies, the biological activities of compounds should span two to three orders of magnitude. But in the present study, the range of antimicrobial activities of the synthesized compounds is within one order of magnitude. This is in accordance with results (Bajaj *et al.*, 2005) where it is stated that the reliability of the QSAR model lies in its predictive ability, even though the activity data are in the narrow range. When biological activity data lie in the narrow range, the presence of minimum standard deviation of the biological activity justifies its use in QSAR studies (Narasimhan *et al.*, 2007). The minimum standard

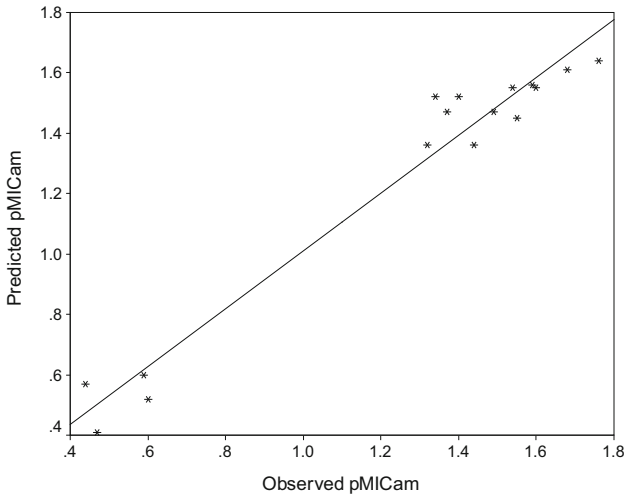

Fig. 3 Plot of observed $\mathrm{pMIC_{am}}$ against predicted $\mathrm{pMIC_{am}}$ by Eq. 3

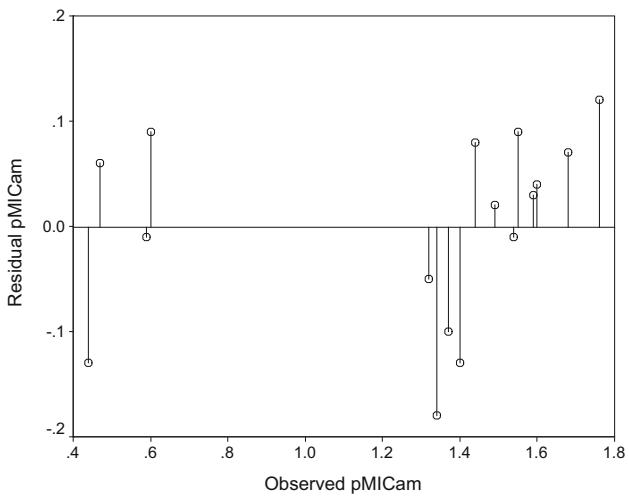

Fig. 4 Plot of observed $\mathrm{pMIC_{am}}$ against residual $\mathrm{pMIC_{am}}$ by Eq. 3

deviation (Table 2) observed in the antimicrobial activity data justifies its use in QSAR studies.

Conclusion

In the present study, a series of 4-hydroxy-3-[1-{(2-hydroxy-aryl) imino}-ethyl]-6-methyl-pyran-2-one (**1**–**4**) and their organosilicon(IV) complexes (**5**–**16**) was synthesized, characterized and screened for its in vitro antimicrobial activity and performed QSAR studies. Antimicrobial studies showed that organosilicon(IV) complexes were found to be more potent than their respective ligands, thus exhibiting their broad spectrum nature and can become a novel antimicrobial agent after further biological studies. The QSAR studies of **1**–**16** reveal the importance of topological parameters, valence first- and third-order molecular connectivity indices ($^{1}\chi^{v}$ and $^{3}\chi^{v}$) in describing the antibacterial and antifungal activity.

Compliance with ethical standards

Conflict of interest The authors declare that they have no conflict of interest.

Human and animal rights statement This article does not contain any studies with human participants or animals performed by any of the authors.

Informed consent Informed consent was obtained from all individual participants included in the study.

References

Abad ZH, Wahab EI, EI-Sarrag MR (2004) Derivatives of phosphate Schiff base transition metal complexes: synthesis, studies and biological activity. Spectrochim Acta A 60:271–277

Bajaj S, Sambi SS, Madan AK (2005) Prediction of anti-inflammatory activity of *N*-arylanthranilic acids: computational approach using refined Zagreb Indices. Croat Chem Acta 78:165–174

Balaban AT (1982) Highly discriminating distance based topological indices. Chem Phys Lett 89:399–404

Belwal S, Singh RV (2000) Synthetic, spectroscopic and applied aspects of some of the organosilicon(IV) and organotin(IV) complexes. Phosphorus Sulfur Silicon Relat Elem 157:43–56

Bharti SK, Patel SK, Nath G, Tilak R, Singh SK (2010) Synthesis, characterization, DNA cleavage and in vitro antimicrobial activities of copper(II) complexes of Schiff bases containing a 2,4-disubstituted thiazole. Transit Met Chem 35:917–925

Cappucino JG, Sherman N (1999) Microbiology: a laboratory mannual. Addison Wesley Longman Inc, California. p **263**

Devi J, Batra N (2013) Transition metal(II) complexes with nitrogen, oxygen and sulphur (NOS) donor Schiff base hydrazone: synthesis, spectroscopic and antimicrobial studies. Asian J Res Chem 6(10):960–967

Devi J, Batra N (2015) Synthesis, characterization and antimicrobial activities of mixed ligand transition metal complexes with isatin monohydrazone Schiff base ligands and heterocyclic nitrogen base. Spectrochim Acta A A135:710–719

Devi J, Batra N, Malhotra R (2012a) Ligational behavior of Schiff bases towards transition metal ion and metalation effect on their antibacterial activity. Spectrochim Acta A 97:397–405

Devi J, Kumari S, Asijaa S, Malhotra R (2012b) Synthetic, spectroscopic, and biological aspects of triorganosilicon(IV) complexes of tridentate Schiff bases. Phosphorus, Sulfur Silicon Relat Elem 187(11):1409–1417

Devi J, Kumari S, Malhotra R (2012c) Synthesis, spectroscopic studies, and biological activity of organosilicon(IV) complexes of ligands derived from 2-aminobenzothiazole derivatives and 2-hydroxy-3-methoxy benzaldehyde. Phosphorus, Sulfur Silicon Relat Elem 187(5):587–597

Dholakiya PP, Patel MN (2004) Metal Complexes: preparation, magnetic, spectral, and biocidal studies of some mixed-ligand complexes with Schiff bases containing NO and NN donor atoms. Synth React Inorg Met-Org Chem 34:553–563

Golbraikh A, Tropsha A (2002) Beware of q^2! J Mol Graph Model 20:269–276

Hansch C, Fujita T (1964) p–σ–π analysis: a method for the correlation of biological activity and chemical structure. J Am Chem Soc 86:1616–1626

Hansch C, Leo A, Unger SH, Kim KH, Nikaitani D, Lien EJ (1973) "Aromatic" substituent constants for structure-activity correlations. J Med Chem 16:1207–1216

Hyperchem 6.0 (1993) Hypercube, Inc., Florida

Jain M, Gaur S, Diwedi SC, Joshi SC, Singh RV, Bansal A (2004) Nematicidal, insecticidal, antifertility, antifungal and antibacterial activities of salicylanilide sulphathiazole and its manganese, silicon and tin complexes. Phosphorus, Sulfur Silicon Relat Elem 179(8):1517–1537

Judge V, Narasimhan B, Ahuja M, Sriram D, Yogeeswari P, Clercq ED, Pannecouque C, Balzarini J (2012) Isonicotinic acid hydrazide derivatives: synthesis, antimicrobial activity and QSAR studies. Med Chem Res 21:1451–1470

Kier LB, Hall LH (1976) Molecular connectivity in chemistry and drug research. Academic Press, NewYork

Kumar A, Narasimhan B, Kumar D (2007) Synthesis, antimicrobial, and QSAR studies of substituted benzamides. Bioorgan Med Chem 15:4113–4124

Kumar R, Kumar P, Kumar M, Narasimhan B (2012) Synthesis, antimicrobial evaluation, and QSAR studies of 4-amino-3-hydroxy-naphthalene-1-sulfonic acid derivatives. Med Chem Res 21:4301–4310

Lather V, Madan AK (2005) Topological models for the prediction of anti-HIV activity of dihydro(alkylthio) (naphthylmethyl)oxopyrimidines. Bioorgan Med Chem 13:1599–1604

Mahiwal K, Kumar P, Narasimhan B (2012) Synthesis, antimicrobial evaluation, ot-QSAR and mt-QSAR studies of 2-amino benzoic acid derivatives. Med Chem Res 21:293–307

Malhotra R, Mehta J, Puri JK (2007) Heterobimetallic complexes containing iron(II) and hexa-coordinated organosilicon. Cent Eur J Chem 5:858–867

Munde AS, Jagdale AN, Jadhav SM, Chondhekar TK (2010) Synthesis, characterization and thermal study of some transition metal complexes of an asymmetrical tetradentate Schiff base ligand. J Serb Chem Soc 75(3):349–359

Narasimhan B, Judge V, Narang R, Ohlan S, Ohlan R (2007) Quantitative structure activity relationship studies for prediction of antimicrobial activity of synthesized 2,4-hexadienoic acid derivatives. Bioorg Med Chem Lett 21(17):5836–5845

Nejo AA, Kolawole GA, Nejo AO, Adeola A, Gabriel KA, Ayorinde NO (2010) Synthesis, characterization, antibacterial, and thermal studies of unsymmetrical Schiff-base complexes of cobalt(II). J Coord Chem 63:4398–4410

Raman R, Dhaveethu Raja J, Sakthivel A (2007) Synthesis, spectral characterization of Schiff base transition metal complexes: DNA

cleavage and antimicrobial activity studies. J Chem Sci 119:303–310
Randic M (1975) On characterization of molecular branching. J Am Chem Soc 97:6609–6615
Randic M (1993) Comparative regression analysis: regression based on a single descriptor. Croat Chem Acta 66:289–312
Singh K, Dharampal Dhiman SS (2009) Spectral studies and antimicrobial activities of organosilicon(IV) and organotin(IV) complexes of nitrogen and sulfur donor Schiff bases derived from 4-amino-5-mercapto-3-methyl-*s*-triazole. Main Group Chem 8:47–59
SPSS for Windows, version 10.05 (1999) SPSS Inc., Bangalore, India
TSAR 3D Version 3.3 (2000) Oxford Molecular Limited, Oxford
Vogel AI (1999) Text book of quantitative chemical analysis, 5th edn. Longmans, Edison, Wesely, London
Yousef TA, Abu El-Reash GM, El-Gammal OA, Bedier RA (2012) Co(II), Cu(II), Cd(II), Fe(III) and U(VI) complexes containing a NSNO donor ligand: synthesis, characterization, optical band gap, in vitro antimicrobial and DNA cleavage studies. J Mol Struct 1029:149–160